Available online at www.sciencedirect.com
SCIENCE DIRECT®

Journal of the European Ceramic Society 23 (2003) 1509–1515

www.elsevier.com/locate/jeurceramsoc

Influence of SiC infiltration on some properties of porous carbon materials

S. Kluska[a], S. Jonas[a,*], E. Walasek[a], T. Stapinski[b], M. Pyzalski[a]

[a] *University of Mining and Metallurgy, Department of Refractories and Ceramics, al. Mickiewicza 30, 30-059 Krakow, Poland*
[b] *University of Mining and Metallurgy, Department of Electronics, al. Mickiewicza 30, 30-059 Krakow, Poland*

Received 8 February 2002; received in revised form 5 September 2002; accepted 16 September 2002

Abstract

The work concerns the investigation of the microstructure changes of carbon industrial materials of various porosity after the pulse chemical vapour infiltration (PCVI). The authors have focused their study on the initial steps of infiltration method up to 100 pulses. The experimental data indicate the complex nature of infiltration process due to complex geometry of pores in these materials, non-stability of matrix, influence of thermal stresses. At the initial steps of infiltration process, apparent improvement of oxidation resistance can be observed.

Keywords: Carbon; Infiltration; Oxidation; Porosity; SiC

1. Introduction

Chemical vapour deposition technique (CVD) is a powerful method for microstructure modification of porous materials. This method allows to infiltrate composites by metals and high refractory compounds such as carbides, nitrides, borides and oxides.[1] Recently, the Pressure Pulsed Chemical Vapour Infiltration method (PCVI) has been largely applied. In this method the pressure in the reactor is cyclically changed from low to high values sometimes up to thousands times. Pressure variations in the reactor allows to effectively introduce reactive gaseous mixture into the pores and evacuate post reactive gases. The method is applied to densification of ceramic composites in the final stage of their production.[2,3]

The works on the infiltration from gaseous phase deal with two aspects. Firstly, they concern the researches of models describing quantitatively the relation between the technological process parameters and the variations of the materials microstructure.[4–7]

Secondly, they investigate properties of materials for practical applications, which are characterized by maximal densification obtained by high number of infiltration pulses.[8,9] Some theoretical models can be applied only for materials of high thermal stability and simple shape of pores e.g. cylindrical.

The aim of this work was to examine the possibility of application of PCVI method for modification of industrial carbon products by SiC. The authors focused on PCVI process of low number of pulses (up to 100) and related changes of materials microstructure. The phenomena connected with the initial stages of infiltration may determine following densification process. On the other hand, for some applications as corrosion resistance improvements the maximal filing of material is not needed.

2. Experimental methods

The apparatus for pressure pulsed chemical vapour infiltration (PCVI) is presented in Fig. 1. It consists of chemical reagents dosing system, the reactor and post reaction evacuation gas system. Methyltrichlorosilane (MTS) was saturated by the carrier gas (Ar + 10% H_2) at room temperature in the saturator. The mixture of the source gas and carrier gas of known ratio was fed into the vertical reactor in the form of quartz tube,

* Corresponding author. Fax: +48-12-633-1593.
E-mail address: jonas@uci.agh.edu.pl (S. Jonas).

0955-2219/02/$ - see front matter
PII: S0955-2219(02)00358-8

where up to 5 samples can be located. The reactor was evacuated by a pumping system. The apparatus is equipped with a resistance heater and a temperature controller with the accuracy of 1° C. The system of valves and digital timer enabled precise dosing of reagents in each pulse. After specified time the reactive gas and product gases were evacuated from the reactor to 10^{-2} Torr. The total time for one pulse was 7 s. The detailed infiltration process parameters have been collected in Table 1.

For PCVI process high porous carbon and low porous carbon were used as specimens. High porous carbon (type EG) of 22% porosity and low porous carbon (EK type) of 8% porosity were produced by SGL ANGRAPH in the form rectangular tabs ($60\times50\times50$ mm^3). Both types of specimens were typical industrial materials for electromechanical applications. The samples were cut in the parallel and perpendicular directions of industrial moulding.

In this work the following experimental methods of investigation into the changes of the samples microstructure depending on the number of PCVI pulses were used: SEM, EDS, X-rays diffractometry (XRD), ultrasounds propagation velocity, helium pycnometry, mercury porosimetry and BET. Chemical resistance to oxidation was done both in CO_2 Genevans method according to standard CT C∋B 6161-88 and in air at 1000 °C in atmospheric pressure. The investigations into thermal stability of specimens took place in $Ar + H_2$ gas mixture at 1100 °C.

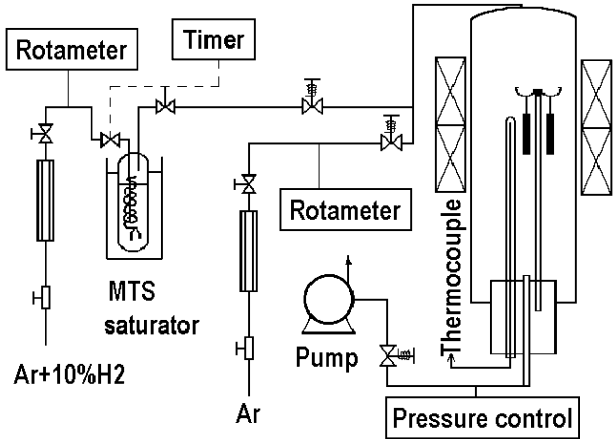

Fig. 1. The apparatus for pressure pulsed chemical vapour infiltration (PCVI) method.

Table 1
Parameters of PCVI process applied during the infiltration

Pressure Ar (hPa)	917
Pressure H_2 (hPa)	90
Pressure CH_3SiCl_3 (hPa)	5
The range of pressure variations (hPa)	1013.25 ÷ 0.1
Flow Ar + 10% H_2 (sccm)	1080
Time of one pulse (sec)	7
Temperature (°C)	1090 ÷ 1100
Number of pulses	30 ÷ 100

3. Microstructure

SEM images and microanalysis of EG type carbon block cross-sections revealed the presence of SiC spherulites which consisted of 3C–SiC, 6H–SiC and 2H–SiC polytypes is analysed by XRD. In Fig. 2 the cross-section of EG carbon after 40 infiltration pulses is shown. One can observe SiC spherulite forms (several micrometeres in diameter) located inside the pores. The dimensions of these forms are about several micrometers. The deposition process of SiC took place both inside the pores and on their surface. This effect is apparently seen after a long time annealing of infiltrated specimens in oxidising atmosphere. Oxidation resulted in the removal of carbon from the matrix. Fig. 3 presents the microscope image of specimen after oxidation.

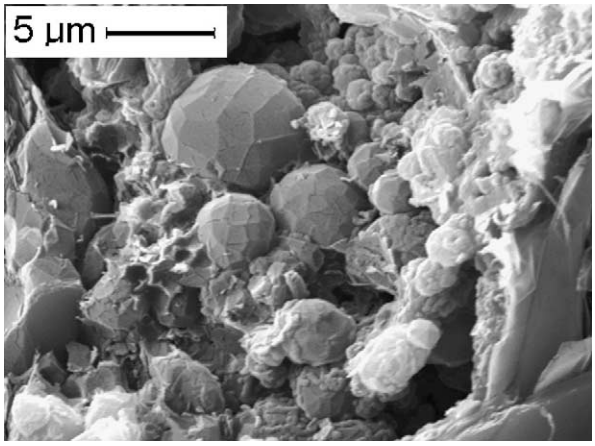

Fig. 2. Spherulities forms of SiC inside the open pores in EG type carbon.

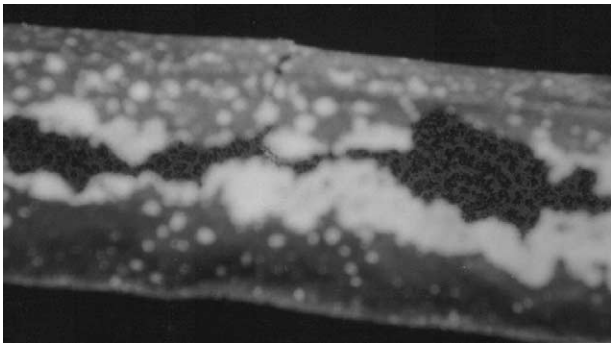

Fig. 3. Optical microscope image (10×) after the total oxidation of carbon in infiltrated EG type specimen (100 pulses). Dark areas correspond to empty places after carbon oxidation. On the surface one can see cracked SiC layer partially oxidised to SiO_2, with covered sample interior. Inside one can see a "skeleton" of open pores filled by SiC in PCVI (light area).

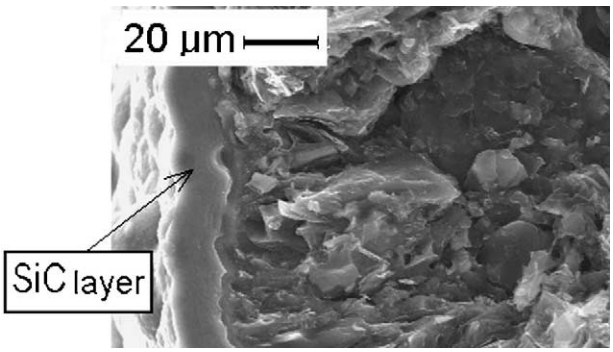

Fig. 4. SEM image of the cross-section of EK type carbon specimen after 100 PCVI pulses. An arrow indicates SiC local layer on the carbon matrix surface.

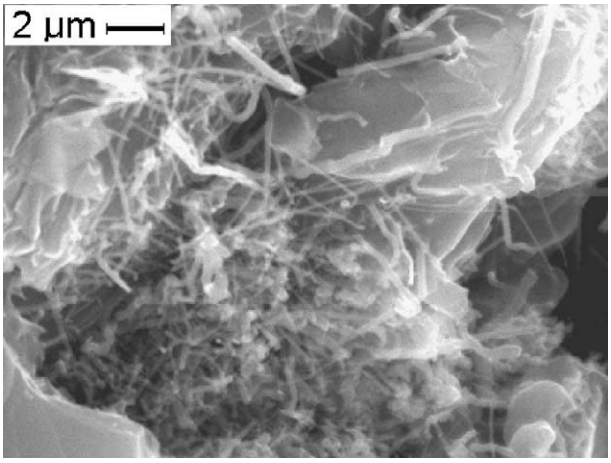

Fig. 5. Nanofibres located into open pores in EK type specimen.

A low porous EK carbon exhibits quite different morphology from EG ones. The formation of SiC took place mainly on the surface of the specimens. Fig. 4 shows a chosen part of sample surface where locally the continuous layer was observed. This process led to the creation of a layer, which was partially blocking the penetration of gaseous reagents into the interior of the specimen and the evacuation of post reactive gases. The confirmation of such mechanism is the appearance of SiC nanofibers inside the pores at some depth from the sample surface (Fig. 5). The experiments show that such longitudinal forms are created in CVD process in conditions of low supersaturation of the gaseous substrates at the surface[10] or in depth.[11] In the explored system, the supersaturation is low due to low penetration of gases into the matrix.

The influence of the microstructure changes on ultrasound propagation velocity was observed. For both types of specimens (EG and EK type) the ultrasound propagation velocity before the PCVI process was examined. After a chosen number of infiltration pulses the velocity was measured for EG and EK samples. Fig. 6 presents the dependence of ultrasound velocity variations vs. the number of infiltration pulses. The results showed the complex nature of phenomena during the infiltration. For low porous EK specimens only a small increase in velocity of about 10 m^{-1} s, comparable with the accuracy of the method, was detected. High porous EG specimens revealed evident increase in propagation velocity, which indicates that the infiltration process is more efficient. The increase in velocity is not monotonic and indicates the complex variation of the microstructure. The presented curves (Fig. 6) for parallel and perpendicular orientation in respect to industrial moulding revealed the apparent increase in velocity for both materials. However, one can observe that for low number of pulses perpendicular velocity is lower than parallel one. As the number of pulses increases, the differences between the velocities for both directions decreases.

The initial steps of the PCVI process led to apparent changes of matrix density. In Table 2 the results of

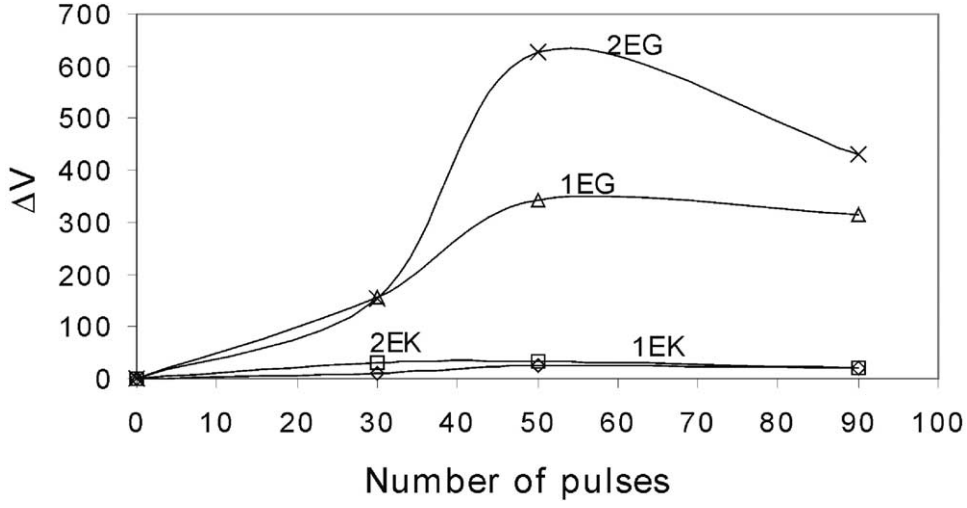

Fig. 6. The dependence of ultrasounds propagation velocity variations ΔV on the number of pulses. 1EG, 1EK—perpendicular orientation; 2EG, 2EK—parallel orientation.

helium density for non-infiltrated and infiltrated EG and EK specimens are presented. After the 30 pulses for both materials, one can observe a small increase in density values and after 100 pulses a consequent small decrease.

The investigation into the dimensions of pores by means of porosimetry of both types of specimens for a chosen number of infiltration pulses are presented in Fig. 7a and b. The apparent decrease in average pores radius after 50 infiltration pulses either for EK or EG type was observed (Fig. 7a and b, curve 2). For example in low porous carbon the radius decreased 4 times in comparison to initial material. The increase in number of infiltration pulses to 90 caused an increase in radius and the shift of the distribution curve to higher values (Fig. 7a and b, curve 3). However, radius values were lower than for initial material (Fig. 7a and b, curve 1). This trend is observed for both EK and EG type specimens.

Table 2
Helium density of infiltrated materials

Material	Helium density (g/cm^3)		
	Non-infiltrated	30 Pulses	100 Pulses
EG ⊥	2.063±0.015	2.085±0.009	2.068±0.005
EG II	2.148±0.012	2.184±0.013	2.152±0.009
EK ⊥	1.961±0.004	1.977±0.012	1.828±0.013
EK II	1.934±0.022	1.985±0.008	1.937±0.006

4. Infiltration and related phenomena

All the obtained results concerning the variations of microstructure during the initial steps of infiltration indicate the complexity of processes and their differences in respect to the porosity of material. Carbon matrix as non-model material is characterised by a complex shape and dimensions of pores, complex geometry of surface and non-uniformity of phase composition. The description of process of infiltration for carbon matrix system is difficult and the existing and well-known models for flat surface or cylindrical surfaces[4,7] for such system cannot be applied. In Fig. 8 one can see the exemplary image of the surface of carbon sample with typical cross sections of pores characterised by numerous necking down. In such a system PCVI deposited material, the reduction of area intersection of necking and the creation of bridges and finally the closure of pores, are presented schematically in Fig. 9.

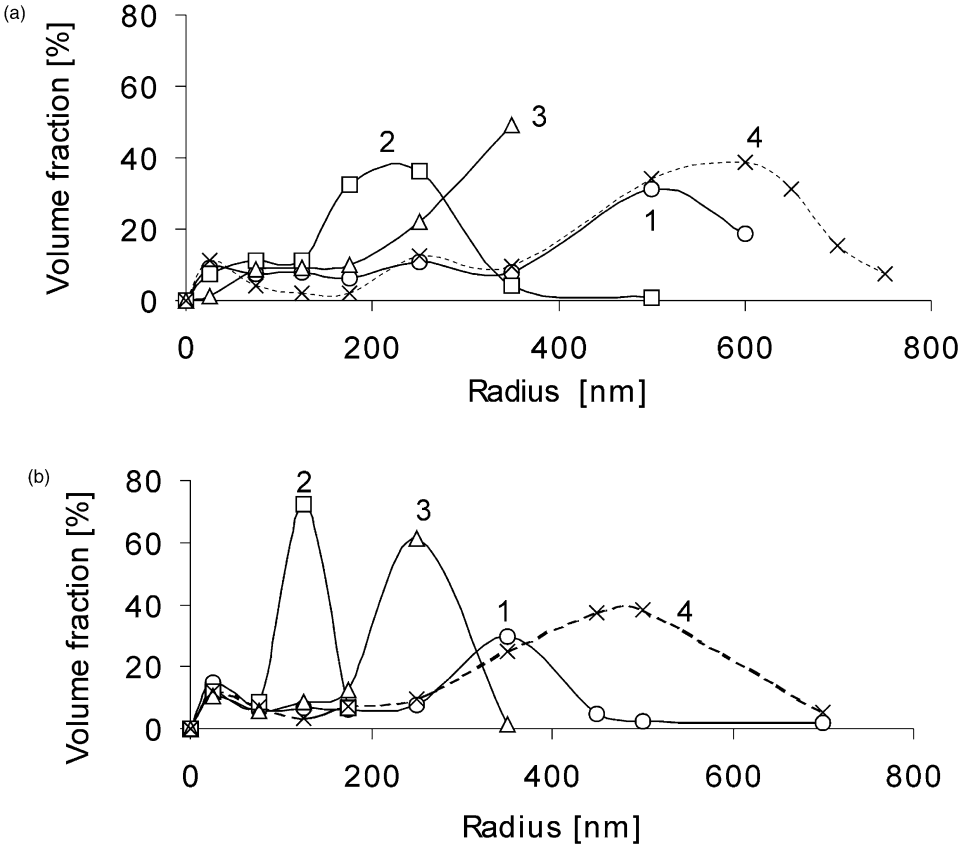

Fig. 7. Pores dimension distribution obtained by means of porosimetry for (a) EG, (b) EK type carbon. The curves numbers indicate: (1) non infiltrated material; (2) infiltrated after 50 pulses; (3) infiltrated after 90 pulses; (4) non infiltrated material after heat treatment.

Microscopic observations confirm the presence of this effect and one can see the formation of SiC bridges connecting the walls of pores, Fig. 10. Such an effect is unfavourable for infiltration process and causes generation of closed pores in the specimen. This effect was confirmed by investigations into closed porosity of EK type carbon. The results are collected in Table 3. After 50 pulses one can observe the apparent increase of about 6% in closed porosity, whereas after 90 pulses a decreases is noticed. These changes as well as the pores dimension distribution variations (Fig. 7b) indicate that the partial opening of pores occurs and is due to thermal expansion mismatch between carbon matrix and deposited SiC ($\alpha_C = 4\times10^{-6}$ K^{-1} and $\alpha_{SiC} = 5.8\times10^{-6}$ K^{-1} at 1250 °C respectively). The thermal stresses result in formation of micro-cracks in SiC layer and destruction of the SiC bridges (see Fig. 10). The above mentioned phenomena are influenced by the nonstability of carbon matrix, matrix degassing, possible graphitisation and etching. These effects lead to reclaimed changes of microstructure, e.g. pores dimension distribution. In Fig. 7a and b dashed curves denote pores distribution for non-infiltrated material after heat treatment in $Ar + 10\%H_2$ at 1100 °C. The increase in pore dimensions can be observed.

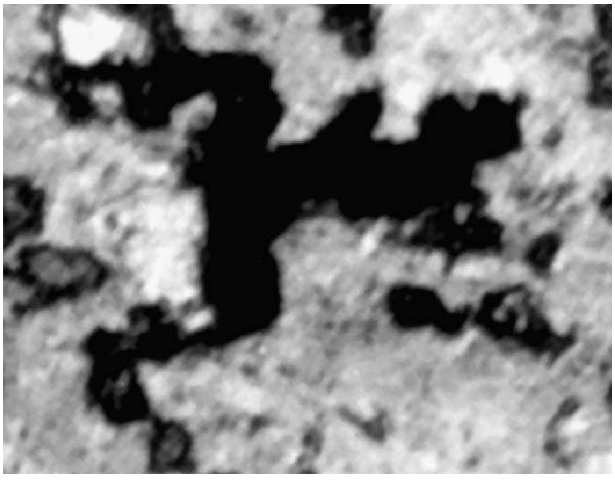

Fig. 8. Cross-section of EG carbon material (optical microscope, 200×).

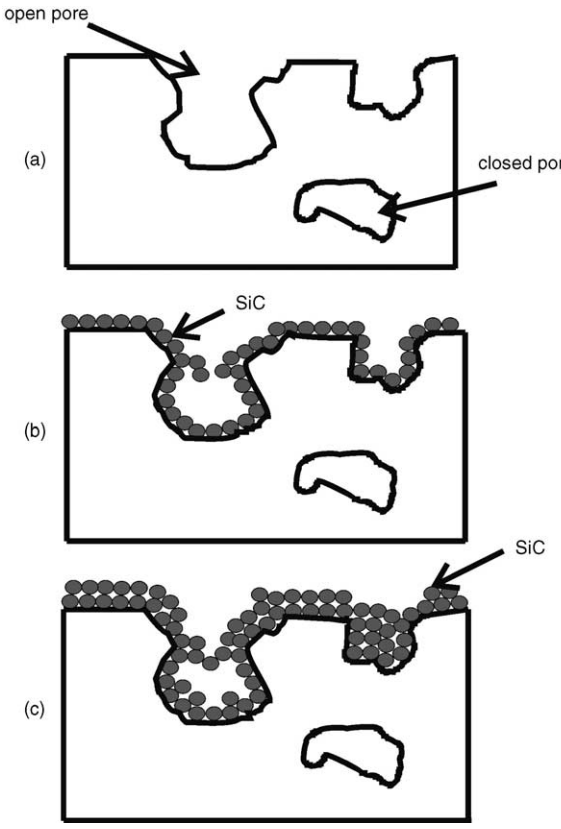

Fig. 9. The illustration of the formation of SiC bridges during PCVI process for materials of complex geometry of pores: (a) carbon matrix, (b) initial steps of infiltration, (c) closure of open pore by SiC bridge.

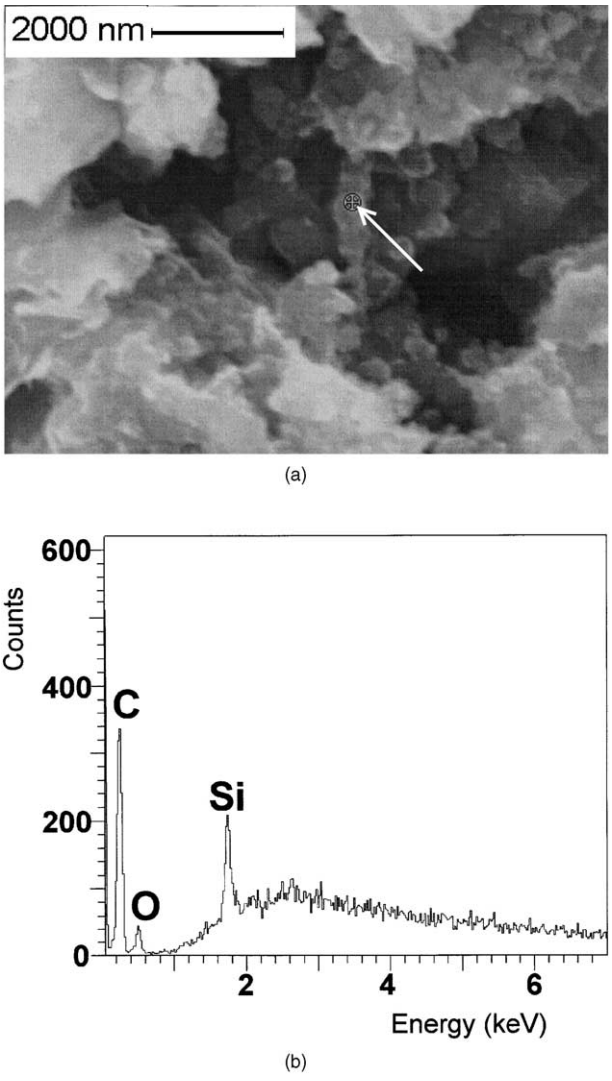

Fig. 10. SEM image of SiC bridges inside open pores connecting opposite walls of pores (a); EPMA spot analysis in place indicated by arrow in SEM image (b).

The variations of the radius distribution due to infiltration (Fig. 7a and b) are influenced by two phenomena: chemical nonstability of carbon matrix and thermal stress. For the evaluation of samples chemical stability of EK and EG type non-infiltrated specimens were annealed in $Ar + H_2$ gaseous mixture at 1100 °C. The porosimetry investigations of these specimens are presented in Fig. 7a and b, curve 4 and revealed a shift of radius to higher values and increase in total open porosity in respect to non annealed carbon samples. One can conclude that the observed increase in average pore radius and volume fraction (Fig. 7a and b, curve 4) is due to the etching process of carbon matrix by hydrogen. During the PCVI process which takes place at 1100 °C in the reactive mixture $MTS + Ar + 10\%H_2$ the uncovered by SiC surface of carbon matrix is etching. The increase in mean radius of pores (Fig. 7a and b, curve 3) is the confirmation of etching process.

5. Chemical resistance

Chemical resistance to oxidation was done with a flow of CO_2 equal 180 sccm and enables us to determine the reaction coefficient K for all materials given by:

$$K = \frac{vT}{mT_1} R$$

where v is CO_2 flow rate, T—sample temperature during oxidation and T_1 temperature of CO_2 in the gas inlet, m carbon mass in the sample and R degree of reaction of gas with the sample CT C∋B 6161-88. The experiment was done at $T = 1000$ °C and $T_1 = 25$ °C.

The investigations of samples in CO_2 atmosphere revealed different values of reaction coefficient K for low and high porosity carbon before the infiltration and after a given number of pulses. The results are collected

Table 3
Changes of closed porosity for EK samples after the chosen number of pulses

Material	Closed porosity (%)		
	Non-infiltrated	50 Pulses	90 Pulses
EK ⊥	15.4±0.2	21.6±0.2	20.5±0.2

Table 4
Reactivity results of carbon specimens after oxidation in CO_2

Material	Reactivity coefficient K ($cm^3/g{\cdot}s$)	Ash content (mass %)	Volatile products (mass %)
EG non-infiltrated	0.12	0.25	0.30
EG 100 pulses	0.00	–	–
EK non-infiltrated	0.11	7.50	0.30
EK 100 pulses	0.01	–	–

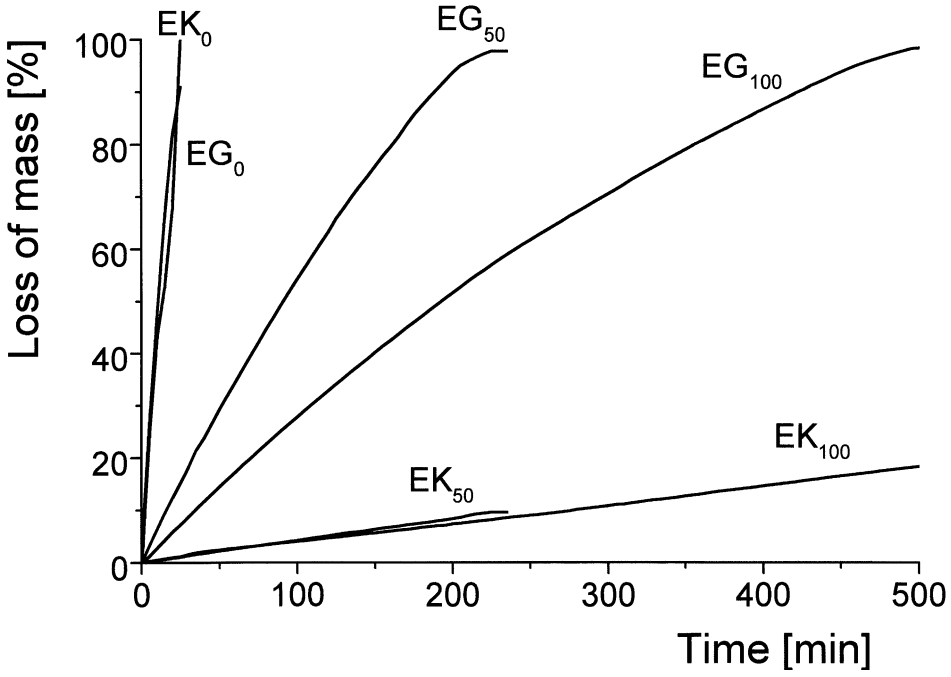

Fig. 11. Mass loss vs. annealing time for EK and EG type carbon. Numbers denote the proper number of infiltration pulses. EK_{100} after 100 pulses, EG_{100} after 100 pulses, EK_{50} after 50 pulses, EG_{50} after 50 pulses, EK_0 and EG_0.

Table 5
Linear correlation of the relation of mass loss versus time for EG and EK specimens

Material	Linear regresion function	
	EG	EK
Non-infiltrated	$y=3.6049x+2.2089$	$y=3.7904x+6.4677$
30 Pulses	$y=1.8586x+10.207$	$y=0.0654x-0.1760$
50 Pulses	$y=0.4353x+7.1540$	$y=0.0417x+0.0855$
100 Pulses	$y=0.1955x+8.3995$	$y=0.0358x+0.2903$

x—oxidation time (min). y—mass loss (%). Linear correlation coefficient $R>0.96$.

in Table 4. All specimens after the process of infiltration revealed zero values of reaction coefficient K, which indicates excellent modification of properties of carbon.

The oxidation test in the air led to detection of mass loss of non-infiltrated and infiltrated specimens. Fig. 11 shows the mass loss vs. time for EK and EG type infiltrated (50 and 100 pulses) and non-infiltrated carbon specimens. One can notice the apparent differences in oxidizing rate for both materials. After the first steps of infiltration EK type low porous carbon revealed drastic improvement of oxidation resistance. For EG type specimens this effect is weaker. The differences in oxidation resistance for both materials (Fig. 11) are due to the fact that in low porosity EK type carbon during the infiltration the surface of samples is covered by SiC layer. The modified outer surface by SiC layer is blocking the entrance of oxygen into the sample volume. The small mass loss is due to the discontinuity of SiC layer after the first stages of infiltration process when local oxidation of carbon occurs. For higher number of pulses the SiC layer becomes thicker and continuous, however, some cracks can be observed as the result of stress due to different thermal expansion coefficients.

The infiltration of EG high porous carbon takes place mainly in the whole volume of sample. For low number of pulses (e.g. 50) the major part of the matrix surface is uncovered by SiC and exposed to aggressive action of oxygen. An increase of pulse number has led to an increase in the area of matrix covered by SiC and apparent increase in oxidation resistance.

The experimental data were estimated by the linear function. The slopes of obtained lines are the measure of the oxidation resistance. The values are collected in Table 5.

The presented results cannot be treated like the results of investigation into oxidation kinetics. Carbon–SiC system is rather complex. The oxidation of carbon matrix causes a loss of mass in contrary to oxidation of silicon carbide, which is related to the increase in the mass of the specimen. The measured values are influenced by these oxidation effects. The obtained results estimate only a global behaviour of material in oxidation atmosphere.

6. Conclusions

The initial steps of the infiltration process by PCVI method depends on the type of the carbon matrix. The process is effective for high porous EG type carbon, which was confirmed by the ultrasound measurements, scanning microscopy, porosimetry. In non-model material in applied infiltration conditions the complicated phenomena take place and could not be described on the basis of the existing models. After the low number of the infiltration pulses one can observe a drastical improvement of the oxidation resistance.

References

1. Bertrand, S., Lavaud, J. F., Hadi, R., Vignoles, G. and Pailler, R., The thermal gradient-pulse flow CVI process: a new chemical vapor infiltration technique for the densification of fibre preform. *J. Eur. Ceram. Soc.*, 1998, **18**, 857–870.
2. Ohzawa, Y., Sadanaka, A. and Sugiyama, K., Preparation of gas-permeable SiC shape by pressure-pulsed chemical vapour infiltration into carbonized cotton-cloth preforms. *J. Mater. Sci.*, 1998, **33**, 1211–1216.
3. Sugiyama, K. and Norizuki, K., Preparation of low density free-standing shape of SiC by pressure-pulsed chemical vapour infiltration. *J. Mater. Sci. Lett.*, 1995, **14**, 1720–1722.
4. Fedou, R., Langlais, F. and Naslain, R., A model for the isothermal isobaric chemical vapor infiltration in a straight cylindrical pore. Application to the CVI of SiC. *J. Mat. Syn. Proc.*, 1993, **1**, 61–73.
5. Sheldon, B. W. and Besmann, T. M., Reaction and diffusion kinetics during the initial stages of isothermal chemical vapor infiltration. *J. Am. Ceram. Soc.*, 1991, **74**, 3046–3053.
6. Skamser, D. J., Model of chemical vapor infiltration using temperature gradients. *J. Mater. Res.*, 1997, **12**, 724–736.
7. Naslain, R., Pailler, R., Bourrat, X. and Vignoles, G., Processing of ceramic matrix composites by pulsed-CVI and related techniques. In *Proceedings of the International Symposium on Novel Synthesis and Process of Ceramics*. Key Engineering Materials, Switzerland, 1999, pp. 359–366.
8. Lu, G. Q., Modelling the densification of porous structures in CVI ceramic composites processing. *J. Mater. Proc. Tech.*, 1993, **37**, 487–498.
9. Gupte, S. M. and Tsamopoulos, J. A., Densification of porous materials by chemical vapor infiltration. *J. Electrochem. Soc.*, 1989, **136**, 555–561.
10. Blocher, J. M., Structure/property/process relationships in chemical vapor deposition CVD. *J. Vac. Sci. Technol*, 1974, **11**, 680–688.
11. Tai, N. and Chen, Ch., Nanofiber formation in the fabrication of carbon/silicon carbide ceramic matrix nanocomposites by slurry impregnation and pulse chemical vapor infiltration. *J. Am. Ceram. Soc.*, 2001, **84**, 1683–1688.